Journal of Materials Chemistry C

RSC Publishing

PAPER

View Article Online
View Journal | View Issue

Cite this: J. Mater. Chem. C, 2013, 1, 3729

Elucidating the smectic A-promoting effect of halogen end-groups in calamitic liquid crystals†

Ian Rupar,[a] Kirk M. Mulligan,[a] Jeffrey C. Roberts,[a] Dorothee Nonnenmacher,[b] Frank Giesselmann[b] and Robert P. Lemieux*[a]

Received 21st March 2013
Accepted 2nd May 2013

DOI: 10.1039/c3tc30534a

www.rsc.org/MaterialsC

Two isometric series of chloro-terminated 5-alkoxy-2-(4-alkoxyphenyl)pyrimidine mesogens **QL8-*m*/*n*** and **QL9-*m*/*n*** ($m + n = 16$), with the chloro-terminated alkoxy chain tethered to either the pyrimidine ring or the phenyl ring, were synthesized and their liquid crystalline properties characterized by polarized optical microscopy and differential scanning calorimetry. Based on the analysis of mesogenic properties and correlations to electrostatic potential isosurfaces calculated at the B3LYP/6-31G* level, we present evidence suggesting that the SmA-promoting effect of chloro end-groups is not due to strong polar interactions at the layer interfaces, as previously postulated in the literature. Instead, the evidence suggests that the SmA-promoting effect is due to the electron-withdrawing effect of the chloro end-group, which should reduce electrostatic repulsion between alkoxy chains and, consequently, increase van der Waals interactions between aromatic cores in the orthogonal SmA phase.

Introduction

Tuning the mesogenic properties of thermotropic liquid crystals that form lamellar (smectic) phases has focused primarily on structural modifications of the rigid aromatic core based on the assumption that lamellar ordering is driven by the amphiphilicity of smectogenic materials,[1] and that variations in van der Waals interactions between aromatic cores should have a pronounced effect on mesogenic properties.[2–4] However, studies have shown that the introduction of various end-groups on one aliphatic chain can also have significant effects on mesogenic properties, although the exploitation of such an approach in the tuning of mesogenic properties has been narrower in scope.[5,6] For example, siloxane end-groups are known to promote the formation of smectic liquid crystal phases by nanosegregating from hydrocarbon segments, forming a so-called "virtual siloxane backbone" in an intercalated bilayer structure.[7] More recently, Goodby *et al.* have shown that bulky segments such as cycloalkyl, bicycloalkyl and adamantyl end-groups suppress the formation of anticlinic smectic phases in antiferroelectric liquid crystals such as MHPOBC.[8] They have also shown that the introduction of a halogen end-group promotes the formation of an orthogonal smectic A (SmA) phase at the expense of nematic (N) and tilted smectic C (SmC) phases in a homologous series of difluoroterphenyl mesogens (*e.g.*, **1** and **2** in Fig. 1);[5] Laschat *et al.* later reported that homologous series of chloro- and bromo-terminated 5-phenylpyrimidine mesogens also form exclusively SmA phases.[9]

We have exploited this unusual SmA-promoting effect in the design of liquid crystals with 'de Vries-like' properties, which undergo a SmA–SmC phase transition with a maximum layer contraction of ≤1%.[10,11] The design of these new materials is based on a concept of frustration between two structural

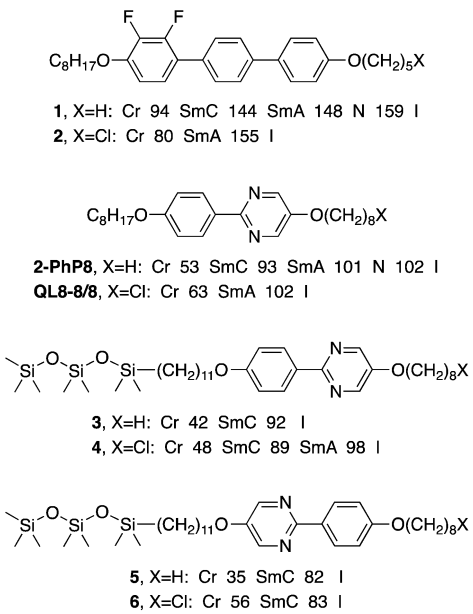

Fig. 1 The effect of a chloro end-group on the mesogenic properties of four different materials; the phase transition temperatures are in °C.[5,10,12]

[a]*Chemistry Department, Queen's University, Kingston, Ontario, Canada. E-mail: lemieux@chem.queensu.ca*

[b]*Institute of Physical Chemistry, Universität Stuttgart, Pfaffenwaldring 55, D-70569 Stuttgart, Germany*

† Electronic supplementary information (ESI) available: Synthetic procedures and structural characterization data. See DOI: 10.1039/c3tc30534a

elements, one promoting the formation of a SmA phase and another promoting the formation of a SmC phase. The design of our first generation of 'de Vries-like' liquid crystals was informed by the results of a model study based on a 5-alkoxy-2-(4-alkoxyphenyl)pyrimidine scaffold, which showed that a siloxane end-group acts as a strong SmC-promoter and confirmed the finding of Goodby *et al.* that a chloro end-group acts as a strong SmA-promoter (see **3** and **QL8-8/8** in Fig. 1). By combining these two elements in the same 2-phenylpyrimidine scaffold, one can obtain mesogens such as **4**, which forms both SmA and SmC phases and undergoes a SmA–SmC phase transition with a maximum layer contraction of 1.6%.[10,12] Interestingly, we also found in this first generation of mesogens that the effect of the chloro end-group is suppressed if the orientation of the 2-phenylpyrimidine core is inverted (*e.g.*, **6** in Fig. 1).

The SmC-promoting effect of the siloxane end-group may be understood in terms of nanosegregation, and the corresponding suppression of out-of-layer fluctuations that reduces the entropic cost of molecular tilt in a supramolecular lamellar structure.[6] However, the origin of the SmA-promoting effect of the chloro end-group is still not well understood. The only explanation presented thus far suggests that this effect "may be due to strong polar interactions at the smectic layer interfaces caused by the terminal halogen units".[5] In this paper, we present evidence that is inconsistent with this explanation based on the mesogenic properties of two isometric series of chloro-terminated 2-phenylpyrimidine liquid crystals **QL8-*m*/*n*** and **QL9-*m*/*n*** ($m + n = 16$). Unlike the more common homologous series, in which the length of a mesogen is gradually increased by adding methylene units to one or both aliphatic chain(s), mesogens in isometric series have the same molecular length but vary in terms of the relative lengths of the aliphatic chains.[13] This experimental approach revealed an apparent synergy between the electron-withdrawing properties of the pyrimidine ring and the chloro end-group in series **QL8-*m*/*n*** that provides the basis of a rationale for the SmA-promoting effect in terms of an increase in electrostatic potential of the chloro-terminated alkoxy chain. We also show the scope of the SmA-promoting effect of halogen end-groups by characterization of the fluoro-, bromo- and iodo-terminated mesogens **QL10-X**.

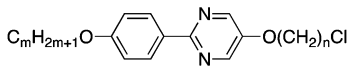

QL8-*m*/*n*

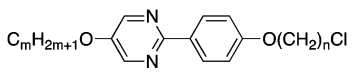

QL9-*m*/*n*

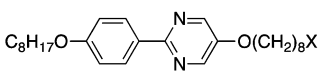

QL10-X: X=F, Br and I

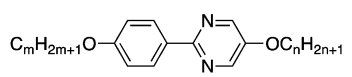

2PhP-*m*/*n*

Results and discussion

Synthesis and characterization

Compounds **QL8-*m*/*n***, **QL9-*m*/*n*** and **QL10-X** were prepared by sequential alkylations of 2-(4-hydroxyphenyl)pyrimidin-5-ol with the appropriate alkan-1-ol and halogen-terminated alkan-1-ol *via* Mitsunobu reactions (see ESI† for detailed synthetic procedures), except for **QL10-I**, which was derived from **QL10-Br** *via* a substitution reaction with NaI in acetone.[14] The new compounds were recrystallized from acetonitrile and hexanes, and analyzed by polarized optical microscopy (POM) and differential scanning calorimetry (DSC). As shown in Table 1, the SmA-promoting effect of the chloro end-group is evident in both isometric series. Compounds in series **QL8-*m*/*n*** form an enantiotropic SmA phase except for **QL8-5/11**, which forms a monotropic SmA phase. The SmA phase formed by these compounds was identified by the formation of characteristic fan textures and dark homeotropic domains on cooling from the isotropic liquid phase, as shown in Fig. 2a. Compounds in series **QL9-*m*/*n*** from $n = 4$ to $n = 8$ form an enantiotropic SmA phase, whereas **QL9-7/9** and **QL9-6/10** form enantiotropic SmA and nematic (N) phases, and **QL9-5/11** forms an enantiotropic nematic phase and a monotropic SmA phase. The nematic phase was identified in all three compounds by the formation of a characteristic Schlieren texture, as shown in Fig. 2b. All three halogen-terminated compounds in series **QL10-X** form an enantiotropic SmA phase, thus demonstrating the generality of the SmA-promoting effect across the entire halogen series. For the purpose of comparison, phase transition temperatures for the corresponding isometric series **2PhP-*m*/*n*** ($m + n = 17$), in which the chloro end-group is substituted with a methyl group,

Table 1 Transition temperatures (°C) and enthalpies of transitions (kJ mol^{-1}, in parentheses) for compounds **QL8-*m*/*n***, **QL9-*m*/*n*** and **QL10-X** on heating

Compound	Cr		SmA		N		I
QL8-12/4	•	72 (41)	•			111 (6.2)	•
QL8-11/5	•	73 (44)	•			112 (8.8)	•
QL8-10/6	•	56 (49)	•			103 (8.1)	•
QL8-9/7	•	51 (25)[a]	•			107 (10)	•
QL8-8/8	•	67 (39)	•			105 (9.2)	•
QL8-7/9	•	48 (10)[b]	•			98 (9.1)	•
QL8-6/10	•	67 (46)	•			95 (10)	•
QL8-5/11	•	93 (57)	(•	85 (9.5))[c]			•
QL9-12/4	•	59 (37)	•			100 (8.3)	•
QL9-11/5	•	65 (42)	•			101 (9.3)	•
QL9-10/6	•	61 (45)	•			97 (8.4)	•
QL9-9/7	•	66 (43)	•			94 (7.5)	•
QL9-8/8	•	76 (28)[d]	•			95 (6.4)	•
QL9-7/9	•	66 (38)	•	82 (1.7)	•	85 (1.0)	•
QL9-6/10	•	72 (39)	•	76 (0.3)	•	85 (1.2)	•
QL9-5/11	•	65 (45)	(•	61 (0.6))[c]	•	76 (1.2)	•
QL10-F	•	47 (9.1)[e]	•			101 (10)	•
QL10-Br	•	52 (27)	•			100 (7.7)	•
QL10-I	•	49 (29)	•			97 (2.8)	•

[a] Preceded by a Cr–Cr transition at 48 °C (19 kJ mol^{-1}). [b] Preceded by a Cr–Cr transition at 38 °C (15 kJ mol^{-1}). [c] Monotropic mesophase. [d] Preceded by a Cr–Cr transition at 72 °C (34 kJ mol^{-1}). [e] Preceded by a Cr–SmX transition at 34 °C (6.8 kJ mol^{-1}).

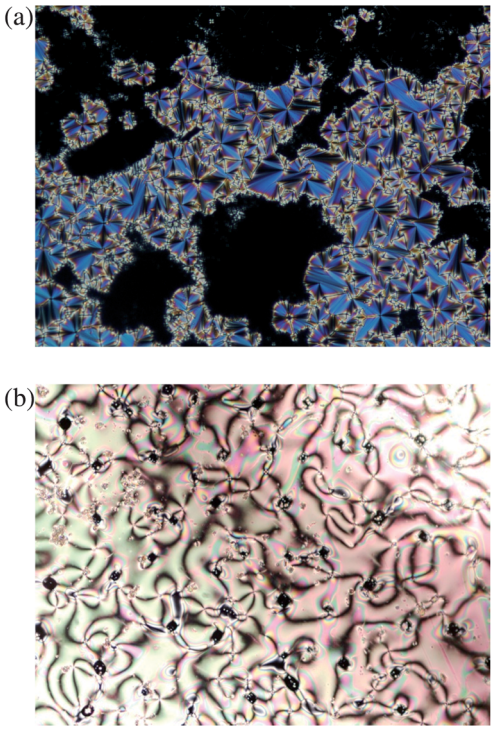

Fig. 2 Polarized photomicrographs of (a) **QL8-9/7** in the SmA phase at 96 °C (top) and (b) **QL9-7/9** in the N phase at 85 °C (bottom) on cooling from the isotropic liquid phase.

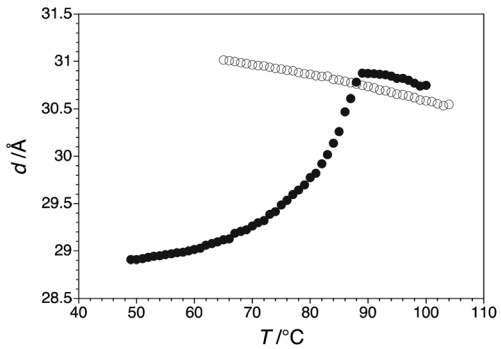

Fig. 3 Smectic layer spacing *d versus* temperature measured on heating from the crystalline phase for compounds **QL8-8/8** (○) and **2PhP-9/8** (●).

were obtained from the patent literature except for compound **2PhP-12/5**, which was synthesized and characterized independently (see ESI†).[15]

Measurements of smectic layer spacings *d* as a function of temperature were carried out by small-angle X-ray scattering (SAXS) for the chloro-terminated compound **QL8-8/8** and the non-chloro analogue **2PhP-9/8.** As shown in Fig. 3, the layer spacing of both compounds exhibits the same degree of negative thermal expansion in the SmA phase, from 30.5 to 31.0 Å for **QL8-8/8** and from 30.7 to 30.9 Å for **2PhP-9/8**, which may be attributed to an increase in the orientational order parameter (S_2).[16] The decrease in layer spacing upon transition to the SmC phase results in a maximum layer contraction of 6.4% for **2PhP-9/8**, which is consistent with the behavior of conventional calamitic smectogens.[17] The *d* values in the SmA phase are near the molecular lengths calculated for **QL8-8/8** (31.8 Å) and **2PhP-9/8** (32.4 Å) as fully extended equilibrium structures minimized at the B3LYP/6-31G* level using Spartan'10 (Wavefunction, Inc., Irvine, CA). This is consistent with a monolayer organization that does not appear to be perturbed by the chloro end-group.

A graphical comparison of the mesogenic properties of **QL8-*m*/*n*** and **QL9-*m*/*n*** isomers (Fig. 4) reveals diagnostic structure–property relationships: (i) the mesogenic properties of **QL8-*m*/*n*** and **QL9-*m*/*n*** are most similar with the chloro end-group positioned in close proximity to the core (*viz.*, **QL8-12/4** and **QL9-12/4**), and (ii) are most dissimilar with the chloro end-group positioned far away from the core (*viz.*, **QL8-5/11** and **QL9-5/11**); (iii) the SmA-promoting effect is evident throughout the **QL8-*m*/*n*** series, in which the chloro-terminated alkoxy chain is tethered to the pyrimidine ring, whereas (iv) the SmA-promoting effect gradually vanishes in the **QL9-*m*/*n*** series, in which the chloro-terminated alkoxy chain is tethered to the phenyl ring, as the distance between the chloro end-group and the core increases. Interestingly, the **QL9-*m*/*n*** and **2PhP-*m*/*n*** series show similar structure-property trends, if one makes no distinction between SmA and SmC phases; in the extreme cases of **QL9-6/10** and **QL9-5/11**, the mesogenic properties are more or less the same as those of the non-halogenated analogues **2PhP-11/6** and **2PhP-12/5.**

The difference in mesogenic properties between **QL8-*m*/*n*** and **QL9-*m*/*n*** is inconsistent with the hypothesis that strong polar interactions between chloro end-groups at the smectic layer interface are responsible for the SmA-promoting effect since any such interaction should be invariant of the

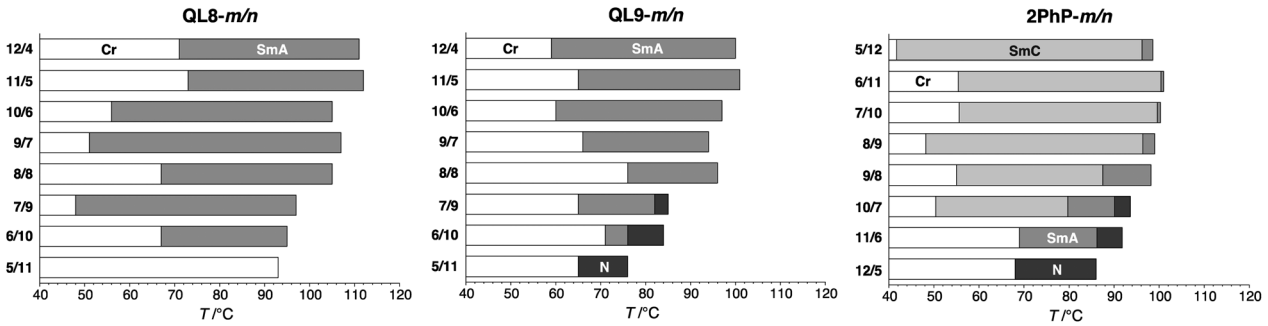

Fig. 4 Mesophases formed by compounds **QL8-*m*/*n***, **QL9-*m*/*n*** and **2PhP-*m*/*n*** on heating.

orientation of the 2-phenylpyrimidine core in relation to the chloro-terminated alkoxy chain. This is particularly evident when one considers that the two isomers with the most dissimilar mesogenic properties are those with the chloro end-group positioned furthest from the core. On the other hand, the fact that the SmA-promoting effect is more consistent in the **QL8-*n*/*m*** series suggests that an effect resulting from a synergy between the pyrimidine ring and the chloro end-group contributes to the stabilization of the SmA phase.

Molecular dipole moments

In analyzing structure–property relationships, we first sought to measure molecular dipole moments μ for **QL8-*m*/*n*** and **QL9-*m*/*n*** to determine if any correlation exists between μ and the mesogenic properties. Fully extended equilibrium structures were minimized at the B3LYP/6-31G* level using Spartan'10, and molecular dipole moments were calculated at the same level of theory. As shown in Fig. 5, molecular dipole moments in series **QL8-*m*/*n*** are significantly smaller than in series **QL9-*m*/*n*** due to the difference in orientation of the 2-phenylpyrimidine core relative to the terminal C–Cl bond. The dipole moment in each series also shows an odd-even effect consistent with the alternating orientation of the C–Cl bond relative to the core dipole moment, as shown in Fig. 6. However, for a given chain length parity, the value of μ remains approximately constant in each series.

Neither the difference in μ between **QL8-*m*/*n*** and **QL9-*m*/*n*** nor the invariance in μ for a given parity in each series correlate with the observed differences in mesogenic properties, as shown in Table 1 and Fig. 4. For example, the isomeric pairs **QL8/QL9-11/5** and **QL8/QL9-5/11** are very different in terms of their relative mesogenic properties, but the two pairs show approximately the same difference in dipole moment ($\Delta\mu = 3.49$ D *vs.* 3.43 D, respectively).

Electrostatic potential isosurfaces

Given that the pyrimidine ring and the chloro end-group are both electron-withdrawing, we then sought to measure their combined effect on the electrostatic potential of the alkoxy chains in series **QL8-*m*/*n*** by calculating electrostatic potential isosurfaces for the extreme isomers **QL8-12/4** and **QL8-5/11** and the intermediate isomer **QL8-8/8**, and by comparing their isosurfaces to those calculated for the corresponding isomers in series **QL9-*m*/*n*** and **2PhP-*m*/*n***. The electrostatic potential isosurface of a molecule displays the electrostatic potential energy (U) of a positive charge along an electron density isosurface according to a spectral color scale ranging from red (negative U) to blue (positive U), and thus gives a three-dimensional representation of molecular charge distribution.

Fully extended equilibrium structures were minimized at the B3LYP/6-31G* level using Spartan'10, and electrostatic potential isosurfaces were calculated at the same level of theory. The isosurfaces shown in Fig. 7 for the three intermediate isomers **QL8-8/8**, **QL9-8/8** and **2PhP-8/9** display electrostatic potentials over the same dynamic range using a symmetrical color scale from red (−155 kJ mol^{-1}) to blue (+155 kJ mol^{-1}), which is based on the highest absolute value of U calculated for these three molecules. The isosurfaces reveal the strong electron-withdrawing effect of the pyrimidine ring—as evidenced by the light blue shading of the methylene group proximal to each pyrimidine ring—and the non-polar character of unsubstituted

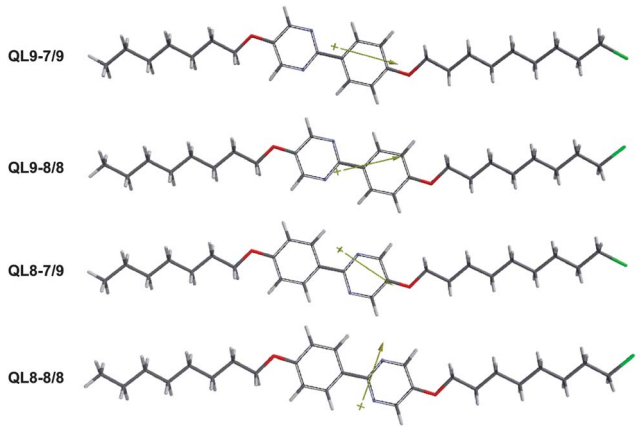

Fig. 6 Molecular structures and dipole moment vectors μ (in yellow) for the isomeric pairs **QL8/QL9-7/9** and **QL8/QL9-8/8** showing the alternation of μ with the parity of the chloro-terminated alkoxy chain length.

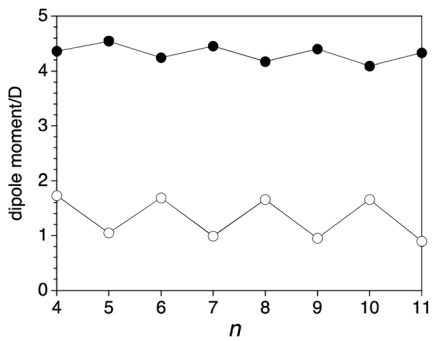

Fig. 5 Molecular dipole moment μ calculated for **QL8-*m*/*n*** (○) and **QL9-*m*/*n*** (●) at the B3LYP/6-31G* level as a function of the chloro-terminated alkoxy chain length n.

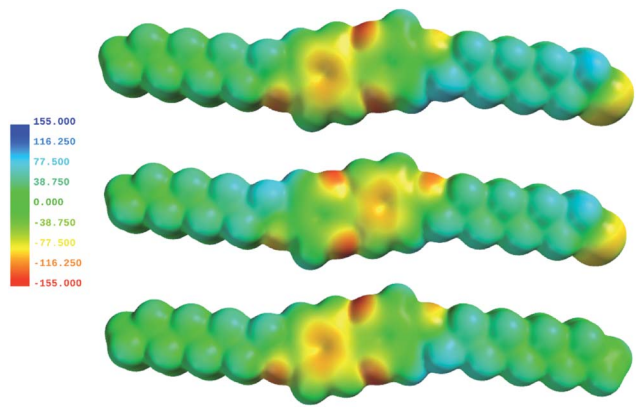

Fig. 7 Electrostatic potential isosurfaces calculated at the B3LYP/6-31G* level for **QL8-8/8** (top), **QL9-8/8** (middle) and **2PhP-8/9** (bottom). The color scale is displayed to the left and ranges from red (−155 kJ mol^{-1}) to blue (+155 kJ mol^{-1}).

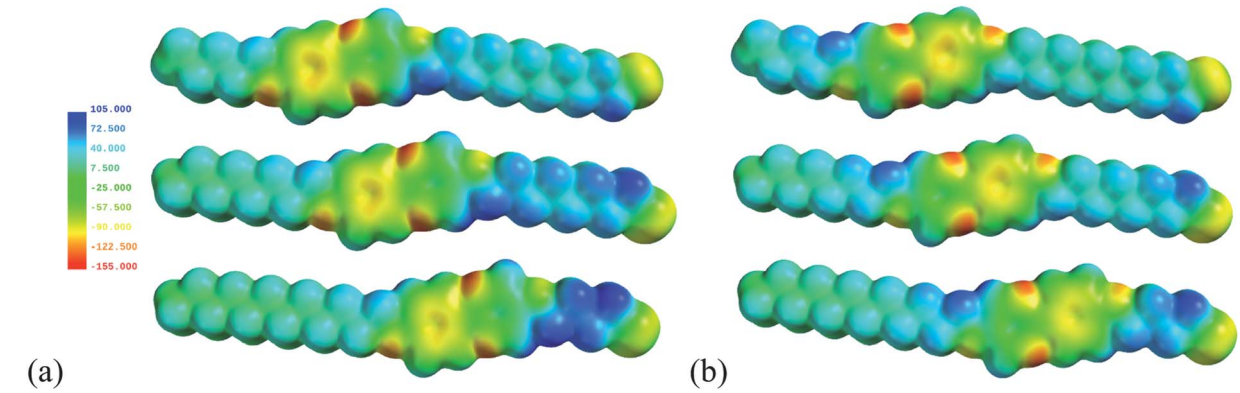

Fig. 8 Electrostatic potential isosurfaces calculated at the B3LYP/6-31G* level for (a) **QL8-5/11** (top), **QL8-8/8** (middle) and **QL8-12/4** (bottom); and (b) **QL9-5/11** (top), **QL9-8/8** (middle) and **QL9-12/4** (bottom). The color scale is displayed to the left and ranges from red (−155 kJ mol^{-1}) to blue (+105 kJ mol^{-1}).

alkoxy chains tethered to a phenyl ring. The isosurfaces also reveal the combined effect of the pyrimidine ring and chloro end-group, which results in higher (more positive) electrostatic potentials in the substituted alkoxy chain of **QL8-8/8;** the effect of the chloro end-group on the substituted alkoxy chain of **QL9-8/8** is also evident, albeit less pronounced given that it is tethered to the phenyl ring.

In order to highlight the electron-withdrawing effect of the pyrimidine ring and chloro end-group in the electrostatic potential isosurfaces of **QL8-*m*/*n*** and **QL9-*m*/*n*** in relation to those of the unsubstituted **2PhP-*m*/*n***, we moved the positive end of the color scale in Fig. 8 and 9 to the highest positive U value calculated in the three series, which decreases the dynamic range of U (−155 kJ mol^{-1} to +105 kJ mol^{-1}) and offsets the color scale. Once again, the combined effect of the pyrimidine ring and chloro end-group in series **QL8-*m*/*n*** can be seen in Fig. 8, resulting in higher electrostatic potentials than those calculated for the corresponding isomers in series **QL9-*m*/*n***. The effect of the chloro end-group on U becomes more pronounced as the distance between the core and chloro-end group decreases, which correlates qualitatively with the SmA-promoting effect of the latter in both series **QL8-*m*/*n*** and **QL9-*m*/*n***. Notwithstanding the apparent synergy between the pyrimidine ring and chloro end-group, the calculations do reveal a measurable shift towards higher electrostatic potentials in the chloro-terminated alkoxy chains of both **QL8-*m*/*n*** and **QL9-*m*/*n*** relative to the non-chloro analogues **2PhP-*m*/*n*** (see Fig. 9), except perhaps in the case of **QL9-5/11**, which displays an electrostatic potential isosurface that is qualitatively very similar to that of **2PhP-12/5**. This similarity is consistent with the fact that both compounds exhibit very similar mesogenic properties.

Assuming an antiparallel organization of mesogens in the smectic layers, the effect of a more positive electrostatic potential in one of the alkoxy chains should be to reduce electrostatic repulsion between side-chains. But how can this favor the orthogonal SmA phase over the tilted SmC phase? In homologous mesogenic series, the lengthening of alkyl chains normally favors the SmC phase over the SmA phase by virtue of an increase in 'entropic pressure' associated with the conformational disorder of alkyl chains.[12] Longer chains have more

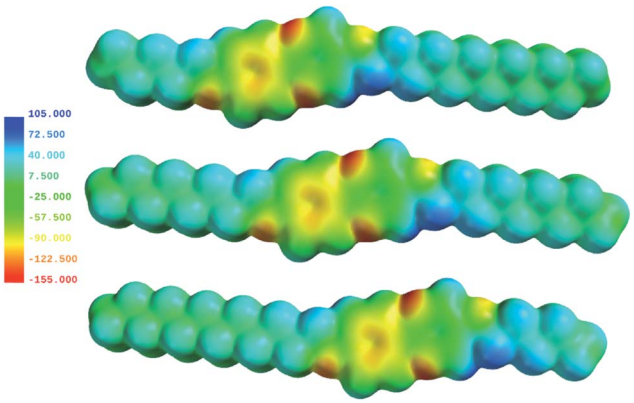

Fig. 9 Electrostatic potential isosurfaces calculated at the B3LYP/6-31G* level for **2PhP-5/12** (top), **2PhP-8/9** (middle) and **2PhP-12/5** (bottom). The color scale is displayed to the left and ranges from red (−155 kJ mol^{-1}) to blue (+105 kJ mol^{-1}).

conformational degrees of freedom than shorter ones and therefore occupy more conformational space, thus forcing rigid aromatic cores farther apart in the diffuse lamellar structure of

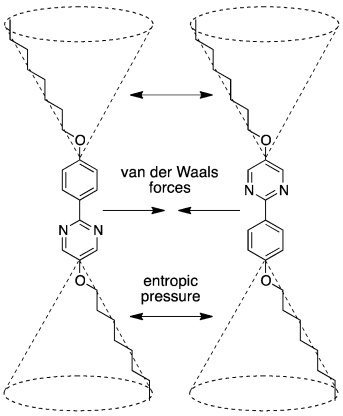

Fig. 10 Graphical representation of the interplay between van der Waals forces and entropic pressure in the SmA phase. The conical volumes approximate the conformational space occupied by the aliphatic chains.

an orthogonal SmA phase.[18] According to this model, free energy is minimized upon tilting in the SmC phase by achieving a balance between the entropic pressure caused by conformational disorder of the alkyl chains and the attractive van der Waals interactions of the aromatic cores (Fig. 10). Tilting also increases the average cross-section of the core to match that of the disordered alkyl chains. In the case of mesogens with chloro end-groups, a reduction in electrostatic repulsion between alkyl chains in the SmA phase should have an effect similar to that of reducing entropic pressure, *i.e.*, to increase attractive core–core interactions to such an extent that the entropic cost of molecular tilt in terms of reduced out-of-layer fluctuations and increased rotational order about the director is prohibitive.

This hypothesis is consistent with the fact the SmA-promoting effect of the chloro end-group is not as pronounced when the alkoxy chain is tethered to the phenyl ring, and decreases with increasing distance between the chloro end-group and the core. It is also consistent with the observed suppression of the SmA phase formed by **4** upon inverting the orientation of the 2-phenylpyrimidine core to give **6**, which results in the chloro-terminated alkoxy chain being tethered to the phenyl ring.[10] Hence, a shift towards more positive electrostatic potentials in alkyl chains may account for the SmA-promoting effect of chloro end-groups, but it may not be the only contributing factor. As shown in Table 1, a comparison of mesogenic properties between **QL8-8/8** and the fluoro-, bromo- and iodo-terminated analogues **QL10-X** shows that the SmA-promoting effect is consistent along the entire halogen series despite the decrease in electronegativity of the halogen group from fluoro to iodo, although the electrostatic potential isosurfaces calculated for **QL10-F** and **QL10-Br** are qualitatively similar to that calculated for **QL8-8/8** (see Fig. S1 in ESI;† we could not minimize **QL10-I** at the B3LYP/6-31G* level using Spartan'10). This may be explained by the corresponding increase in polarizability of the halogen group, which should reduce halogen–halogen repulsion by virtue of stronger dispersive interactions and therefore contribute to further reduction in electrostatic repulsion of the alkoxy chains.

Summary

Based on our analysis of structure–property relationships in two isometric series of chloro-terminated 2-phenylpyrimidine mesogens, and correlations to electrostatic potential isosurfaces calculated at the B3LYP/6-31G* level, we have shown that the SmA-promoting effect of chloro end-groups is not due to strong polar interactions at the layer interfaces, as previously postulated in the literature.[5] Instead, the evidence suggests that the effect is due to the electron-withdrawing effect of the chloro end-group, which should reduce electrostatic repulsion between the alkoxy chains and increase attractive van der Waals interactions between aromatic cores in the SmA phase.

Acknowledgements

We thank the Natural Sciences and Engineering Research Council of Canada and the Deutsche Forchungsgemeinschaft (NSF/DFG *Materials World Network* program DFG Gi 243/6) for support of this work.

References

1 B. I. Ostrovskii, in *Structure and Bonding*, ed. D. M. P. Mingos, Springer-Verlag, Berlin, 1999, vol. 94, pp. 199–240.
2 (*a*) J. W. Goodby, in *Handbook of Liquid Crystals*, ed. D. Demus, J. Goodby, G. W. Gray, H.-W. Spiess and V. Vill, Wiley-VCH, Weinheim, 1998, vol. 2A, pp. 411–469; (*b*) J. W. Goodby, in *Ferroelectric Liquid Crystals: Principles, Properties and Applications*, ed. J. W. Goodby, R. Blinc, N. A. Clark, S. T. Lagerwall, M. A. Osipov, S. A. Pikin, T. Sakurai, K. Yoshino and B. Zeks, Gordon & Breach, Philadelphia, 1991, pp. 99–247.
3 J. W. Goodby, I. M. Saez, S. J. Cowling, J. S. Gasowska, R. A. MacDonald, S. Sia, P. Watson, K. J. Toyne, M. Hird, R. A. Lewis, S.-E. Lee and V. Vaschenko, *Liq. Cryst.*, 2009, **36**, 567–605.
4 M. Hird, *Liq. Cryst.*, 2011, **38**, 1467–1493.
5 J. W. Goodby, I. M. Saez, S. J. Cowling, V. Görtz, M. Draper, A. W. Hall, S. Sia, G. Cosquer, S.-E. Lee and E. P. Raynes, *Angew. Chem., Int. Ed.*, 2008, **47**, 2754–2787.
6 (*a*) C. Tschierske, *Isr. J. Chem.*, 2012, **52**, 935–959; (*b*) C. Tschierske, *J. Mater. Chem.*, 2001, **11**, 2647–2671; (*c*) C. Tschierske, *J. Mater. Chem.*, 1998, **8**, 1485–1508.
7 (*a*) H. J. Coles, H. Owen, J. Newton and P. Hodge, *Liq. Cryst.*, 1993, **15**, 739–744; (*b*) K. Sunohara, K. Takatoh and M. Sakamoto, *Liq. Cryst.*, 1993, **13**, 283–294; (*c*) H. Poths, E. Wischerhoff, R. Zentel, A. Schönfeld, G. Henn and F. Kremer, *Liq. Cryst.*, 1995, **18**, 811–818; (*d*) J. Naciri, J. Ruth, G. Crawford, R. Shashidhar and B. R. Ratna, *Chem. Mater.*, 1995, **7**, 1397–1402; (*e*) J. Z. Vlahakis, K. E. Maly and R. P. Lemieux, *J. Mater. Chem.*, 2001, **11**, 2459–2464.
8 (*a*) S. J. Cowling, A. W. Hall and J. W. Goodby, *Liq. Cryst.*, 2005, **32**, 1483–1498; (*b*) S. J. Cowling and J. W. Goodby, *Chem. Commun.*, 2006, 4107–4109.
9 G. F. Starkulla, E. Kapatsina, A. Baro, F. Giesselmann, S. Tussetschläger, M. Kaller and S. Laschat, *Beilstein J. Org. Chem.*, 2009, **5**, 63.
10 L. Li, C. D. Jones, J. Magolan and R. P. Lemieux, *J. Mater. Chem.*, 2007, **17**, 2313–2318.
11 (*a*) J. C. Roberts, N. Kapernaum, Q. Song, D. Nonnenmacher, K. Ayub, F. Giesselmann and R. P. Lemieux, *J. Am. Chem. Soc.*, 2010, **132**, 364–370; (*b*) Q. Song, D. Nonnenmacher, F. Giesselmann and R. P. Lemieux, *Chem. Commun.*, 2011, **47**, 4781–4783; (*c*) Q. Song, D. Nonnenmacher, F. Giesselmann and R. P. Lemieux, *J. Mater. Chem. C*, 2013, **1**, 343–350.
12 The parent compound **2-PhP8** undergoes a SmA–SmC phase transition with a maximum layer contraction of 7.1%. C. S. Hartley, N. Kapernaum, J. C. Roberts, F. Giesselmann and R. P. Lemieux, *J. Mater. Chem.*, 2006, **16**, 2329–2337.
13 (*a*) J. Malthete, J. Canceill, J. Gabard and J. Jacques, *Tetrahedron*, 1981, **37**, 2815–2821; (*b*) J. Malthete, J. Billard, J. Canceill, J. Gabard and J. Jacques, *J. Phys., Colloq.*, 1976, **37**, C3-1–C3-11.

14 S. Fletcher, A. Ahmad, E. Perouzel, A. heron, A. D. Miller and M. R. Jorgensen, *J. Med. Chem.*, 2006, **49**, 349–357.
15 K. Ohno, M. Ushioda, S. Saito and K. Miyazawa, Eur. Pat. Appl. 0 313 991, 20 October 1988.
16 J. P. F. Lagerwall, F. Giesselmann and M. D. Radcliffe, *Phys. Rev. E: Stat., Nonlinear, Soft Matter Phys.*, 2002, **66**, 031703.
17 J. P. F. Lagerwall and F. Giesselmann, *ChemPhysChem*, 2006, **7**, 20–45.
18 R. A. Reddy, C. Zhu, R. Shao, E. Korblova, T. Gong, Y. Shen, E. Garcia, M. A. Glaser, J. E. Maclennan, D. M. Walba and N. A. Clark, *Science*, 2011, **332**, 72–77.